The Wigner Monte Carlo Method for Accurate Semiconductor Device Simulation

P. Ellinghaus, M. Nedjalkov, and S. Selberherr
Institute for Microelectronics, TU Wien, Gußhausstraße 27–29/E360, 1040 Wien, Austria
E-mail: {ellinghaus | nedjalkov | selberherr}@iue.tuwien.ac.at

***Abstract*—The Wigner equation can conveniently describe quantum transport problems in terms of particles evolving in the phase space. Improvements in the particle generation scheme of the Wigner Monte Carlo method are shown, which increase the accuracy of simulations as validated by comparison to exact solutions of the Schrödinger equation. Simulations with a time-varying potential are demonstrated and issues which arise in devices with an externally applied voltage between the contacts are treated, thereby further advancing the Wigner Monte Carlo method for the simulation of semiconductor devices.**

I. Introduction

The simulation of the time evolution of a wave packet, which captures both particle- and wave-like physical characteristics of an electron, has been touted as an effective tool to study quantum transport in nanoscale semiconductor devices [1]. The Wigner equation allows for the numerical treatment of transient problems, like the evolution of a wave packet, and has garnered interest in the semiconductor device simulation community in recent times [2]–[5]. The latter is ascribed to the fact that the Wigner formalism facilitates the study of quantum transport phenomena, like tunnelling, using a phase space formulation of quantum mechanics. As a consequence, existing classical notions and models, like Boltzmann scattering mechanisms, can be adopted in the Wigner equation. Furthermore, the Wigner equation allows for a seamless transition between the classical and quantum regimes [6], making it particularly well-suited to study transport in mesoscopic semiconductor devices, where both are at play.

The Wigner transform of the density matrix operator yields the Wigner function $f_w(x,p)$. The associated evolution equation for the Wigner function follows from the von Neumann equation for the density matrix, which for the one-dimensional case treated here is

$$\frac{\partial f_w}{\partial t} + \frac{p}{m^*}\frac{\partial f_w}{\partial x} = \int dp' V_w(x, p-p')\, f_w(x,p',t)\,. \quad (1)$$

If a finite coherence length is considered [7], the momentum values are quantized and the integral is replaced by a summation; the semi-discrete Wigner equation results:

$$\frac{\partial f_w}{\partial t} + \frac{\hbar q \Delta k}{m^*}\frac{\partial f_w}{\partial x} = \sum_{q=-K}^{K} V_w(x, q-q', t)\, f_w(x,q',t), \quad (2)$$

where q is now an index which, henceforth, refers to the quantized momentum, i.e. $p = \hbar(q\Delta k)$, with a resolution determined by the coherence length, $\Delta k = \frac{\pi}{L}$. The Wigner potential is defined accordingly as

$$\begin{aligned} V_w(x,q) &\equiv \frac{1}{i\hbar L}\int_{-L/2}^{L/2} ds\, e^{-i2q\Delta k\cdot s}\delta V(s;x)\,; \quad (3)\\ \delta V(s;x) &\equiv V(x+s) - V(x-s)\,. \end{aligned}$$

The Wigner Monte Carlo (WMC) method, used to solve the Wigner equation, is introduced in Section II. An improved particle-generation scheme is discussed, which helps attain high accuracy simulation results – as validated by comparison to exact solutions of the Schrödinger equation. Furthermore, simulations with a time-varying potential are demonstrated. Section III shows how the WMC simulator can be applied to study the evolution of a wave packet in a semiconductor device with an externally applied voltage between the contacts.

II. Wigner Monte Carlo

This section firstly briefly outlines the method applied to solve the Wigner equation, whereafter the particle generation scheme is revisted. The results obtained using the WMC method are then validated by comparison to an exact solution of the time-dependent Schrödinger equation.

A. Method Outline

Equation (1) is reformulated as an adjoint integral equation (Fredholm equation of the second kind) and is solved stochastically using the Monte Carlo method [8], along with the particle-sign technique [9]. The latter associates a + or – sign to each particle, which carries the quantum information of the particle conveyed to it by the Wigner potential. The term on the right-hand side of (1) gives rise to a particle generation term in the integral equation; the statistics governing the particle generation are determined by the Wigner potential (3), which is normalized to unity (denoted by $\tilde{V}_w$).

A generation event entails the creation of two additional particles with complementary signs and momentum offsets q' and q'', with respect to the momentum q of the generating particle. The two momentum offsets, q' and q'', are determined by sampling the probability distributions $V_w^+(x,q)$ and $V_w^-(x,q)$, dictated by the positive and negative values of the normalized Wigner potential ($\tilde{V}_w$), respectively:

$$\begin{aligned} V_w^+(x,q) &\equiv \max\left(0, \tilde{V}_w\right); \quad (4)\\ V_w^-(x,q) &\equiv \max\left(0, -\tilde{V}_w\right). \quad (5) \end{aligned}$$

978-1-4799-5288-5/14/$31.00

The generation events occur at a rate given by

$$\gamma(x) = \sum_q V_w^+(x,q), \tag{6}$$

which typically lies in the order of $10^{15}\,\mathrm{s}^{-1}$. This rapid increase in the number of particles is counteracted by the notion of particle annihilation, which keeps the number of particles under control, thereby making the method computationally feasible also for higher dimensional simulations.

The particle annihilation concept entails a division of the phase space into many cells – each representing a volume $(\Delta x \Delta k)$ of the phase space – within which particles of opposite sign annihilate each other, e.g. in a given cell with P_i particles with a positive sign and Q_i particles with a negative sign, $|P_i - Q_i|$ particles shall remain after annihilation. These particles are regenerated in the cell, each carrying the sign of $P_i - Q_i$.

B. Particle Generation

According to (3), the Wigner potential is anti-symmetric. Therefore, it can be deduced that $V_w^+(\cdot, q) = V_w^-(\cdot, -q)$. This observation allows both distributions to be sampled by a single random number generation – the generated particles will have momentum offsets of q and $-q$ – which is attractive from a computational point of view and also a valid approach, if a sufficiently large number of particles is considered in the simulation (law of large numbers). However, a problem in this approach arises, when the finite range of the q-values, forming the limits of the summation $\pm K$ in (2), are considered: In (3) the variable s, bounded by the finite coherence length L, is transformed to the variable q, which also must be bounded to ensure that the Wigner transform and its inverse are unitary. Therefore, the value of K cannot be chosen freely but is determined by the coherence length:

$$K = \frac{L}{2\Delta s}, \tag{7}$$

where $\Delta s = \Delta x$ is normally chosen to avoid an interpolation between the grids.

The momentum offsets of the newly generated particles should be such that their momenta remain within the set bounds, i.e. $(q + q', q + q'') \epsilon [-K, K]$. The problem arises if particles are generated in pairs with momenta $q \pm q'$, using a single sampling of the distribution function V_w^+ (or V_w^-). To maintain a balance of positive- and negative-signed particles, it seems reasonable to reject both particles and sample the distribution again, until a momentum offset appears which renders both momentum values valid simultaneously. Such a rejection technique clearly influences the statistics. Moreover, the probability for a valid particle pair to be generated decreases, the closer the momentum of the generating particle is to the limit $\pm K$. In such a case, small momentum offsets are more likely to produce a pair of generated particles with valid momenta, thereby unfairly promoting the generation of particles with high momenta and influencing the momentum distribution of the particle ensemble as a whole. Due to this biasing, it becomes less likely for high-momentum particles to dramatically change their momenta and they persist.

The remedy to this systematic biasing is to not reject both generated particles, if one is assigned a momentum which is out of bounds, but rather only regenerate a single momentum offset for the invalid particle. This approach allows high-momentum particles to generate particles with a much lower momentum, which no longer promotes a persistence of high-momentum particles in the k-distribution. By rejecting (and regenerating) only single particles, the balance of positively- and negatively-signed particles is also not disrupted.

Table I. SIMULATION PARAMETERS

x_0 [nm]	σ [nm]	L_{coh} [nm]	Δk [nm^{-1}]	k_0 [nm^{-1}]
-29.5	10	100	π/L_{coh}	$12\Delta k$

The rejection of generated particles with invalid momenta does influence the statistics. However, the value of K, which results for reasonable values of the coherence length L and the mesh-spacing Δs, is large enough to accomodate the particle momenta which can be reasonably expected from a physical point of view. A process which artificially induces the generation of very high-momentum particles, approaching the bound $\pm K$, due to numerics will be exposed and treated in Sec. III.

C. Validation

For validation purposes the exact solution of the time-dependent Schrödinger equation is compared to results obtained by the Wigner Monte Carlo method. An exact solution of the time-dependent Schrödinger equation can be calculated by

$$\psi(x,t) = \int dx' K(x,t;x',t_0)\,\psi(x',t_0), \tag{8}$$

where $K(\cdot)$ is the propagator function associated to the stationary Hamiltonian describing the system and $\psi(\cdot, t_0)$ is the initial condition of the wave function.

As a benchmark problem a wave packet traveling towards a square potential barrier, to its right, within a closed system is considered here. The minimum uncertainty wave packet, which serves as an initial condition, is defined as

$$\psi(x,t_0) = \left(2\pi\sigma^2\right)^{-1/4} e^{-\frac{(x-x_0)^2}{4\sigma^2}} e^{ik_0 z}, \tag{9}$$

with parameters given in Table I. The potential considered here (square barrier) gives rise to analytic expressions for the propagator [10], allowing an exact solution of the Schrödinger equation to be obtained by a numerical integration of (8). This exact solution avoids approximations associated to numerical treatments and serves as a reliable basis for validation of the results obtained by the WMC simulator. The Wigner transform is applied to (9) to obtain the corresponding Wigner function, which serves as an initial condition for the WMC simulation:

$$f(x,m,t_0) = \frac{1}{\pi} e^{-\frac{(x-x_0)^2}{2\sigma^2}} e^{-(m\Delta k - k_0)^2 2\sigma^2}. \tag{10}$$

Fig. 1 compares the solution obtained by the WMC method and the exact solution of the corresponding Schrödinger equation, over a time sequence, for a $4\,\mathrm{nm}$ wide, $0.1\,\mathrm{eV}$ barrier – the mean energy of the wave package is $0.067\,\mathrm{eV}$. The transmitted and reflected components of the wave packet are evident, as supported by the k-distributions in Fig.2. For the first time a truly quantitative match between the stochastic solution of the Wigner equation and an exact solution of the

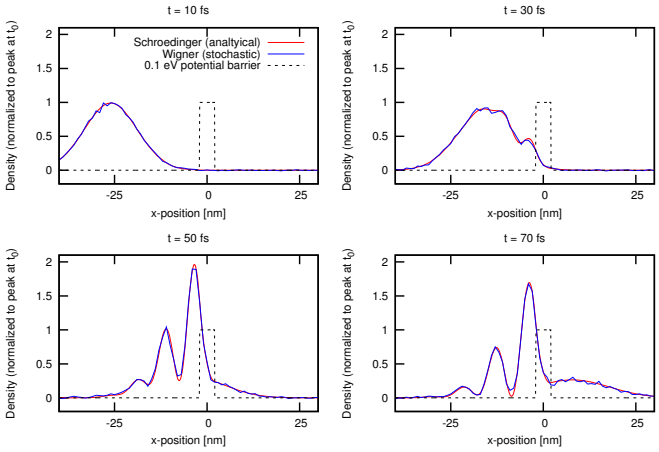

Figure 1. Charge density at various time steps for a wave packet (mean energy of $0.067\,\mathrm{eV}$) approaching a $4\,\mathrm{nm}$ wide, $0.1\,\mathrm{eV}$ high barrier.

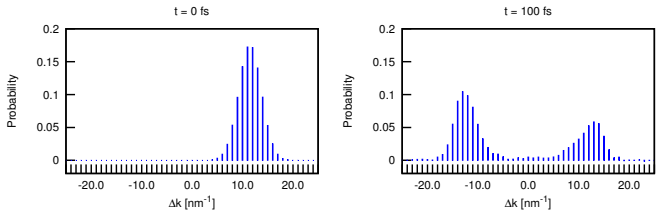

Figure 2. The k-distributions, corresponding to Fig.1, at $0\,\mathrm{fs}$ and $100\,\mathrm{fs}$ showing the reflection and transmission from/through the barrier of a wave packet initially centred around $12\Delta k$.

Schrödinger equation is shown here, thanks to the modified particle generation scheme.

Fig. 3 and Fig. 4 show the result of the same wave package approaching a $0.3\,\mathrm{eV}$ barrier, which leads to almost complete reflection. The simulation required a fine spatial resolution ($0.1\,\mathrm{nm}$) to appropriately represent the sharp edges of the square barrier along with an appropriately chosen coherence length (*cf.* Table I).

Unlike for the discussed analytical method, the inclusion of an arbitrary, time-depedent potential in the WMC simulator is possible, but requires the Wigner potential, V_w, to be recomputed at each time step. The computational cost of the latter can be high (especially in higher dimensions), but can be significantly reduced by using the specialised, box discrete Fourier transform (BDFT) [11], which exploits the correlation between the values of V_w amongst adjacent nodes. As a validation of the WMC results, incorporating a time-dependent potential, the potential barrier is made to rapidly oscillate between $0.04\,\mathrm{eV}$ and $0.1\,\mathrm{eV}$ with a period of $20\,\mathrm{fs}$, and the result is compared to the bounds set by the exact solutions of the limiting (static) cases in the spatial domain, as illustrated in Fig. 5. Fig. 6 shows the k-distributions of the stochastic solutions for the dynamic potential and the two limiting, static potentials – the solution for the oscillating barrier remains within the set static bounds. Moreover, a reflection of the wave packet ($0.067\,\mathrm{eV}$) against the static $0.04\,\mathrm{eV}$ barrier can be identified, which is consistent with the expected quantum behaviour.

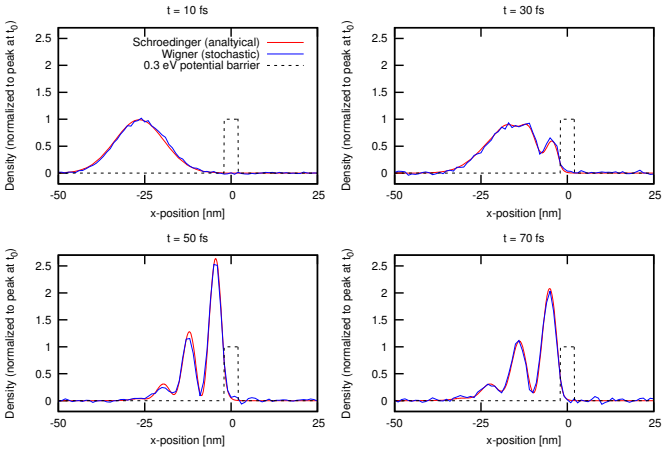

Figure 3. Charge density at various time steps for a wave packet (mean energy of $0.067\,\mathrm{eV}$) approaching a $4\,\mathrm{nm}$ wide, $0.3\,\mathrm{eV}$ high barrier.

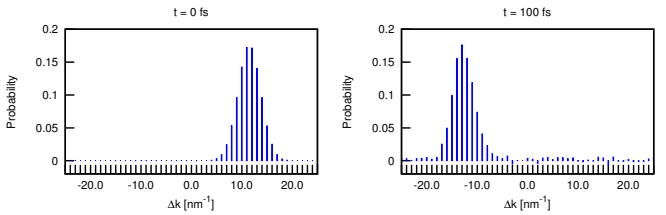

Figure 4. The k-distributions, corresponding to Fig.3, at $0\,\mathrm{fs}$ and $100\,\mathrm{fs}$, showing almost complete reflection from the barrier.

III. Application

The preceding section showed that the WMC simulator produces very accurate results, also for time-varying potentials, which will be encountered when simulating semiconductor devices. This section investigates a more realistic potential profile, as opposed to a square potential barrier.

Fig. 7 shows a wave packet travelling, from the left, along a potential profile suggesting the channel (in transport direction) of a field-effect transistor (FET). The k-distribution (in blue) shows three peaks: the initial distribution (around $12\Delta k$; *cf.* Fig. 2) is split into two parts, one slightly decelerated by the small barrier, the other accelerated by the big potential drop, while the third (smallest) peak suggests a reflection (also seen in the spatial domain) with a change in energy much greater than the potential difference between the left and the right contacts (boundaries). The latter is not physically grounded, but rather a consequence of applying the discrete Fourier transform (DFT) to calculate (3), which implicitly assumes a periodic repetition in the potential profile [12]. The potential difference introduces a discontinuity resulting in a Wigner potential which induces the generation of particles with very high momenta.

The application of a Tukey window function, which smooths the potential towards zero at the limits of the region of coherence, clearly remedies this problem [12] (shown in red in Fig. 7) and also avoids negative 'probabilities' appearing in the k-distribution, leading to more satisfactory, smoother results overall.

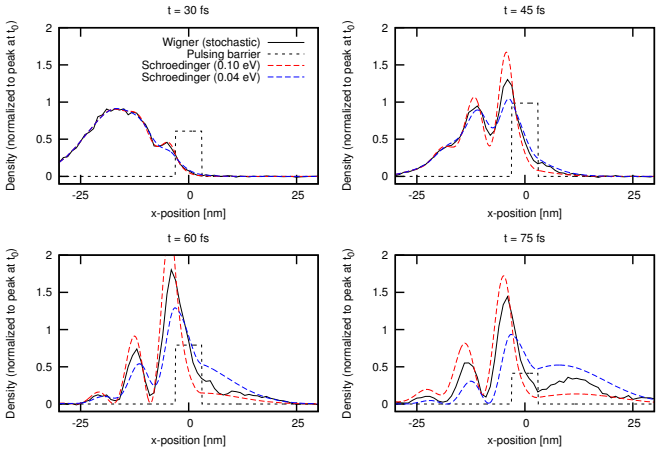

Figure 5. Charge density at various time steps for a 6 nm wide barrier oscillating between 0.04 eV and 0.1 eV. The bounds are given by exact solutions of the Schrödinger equation for the static, limiting cases.

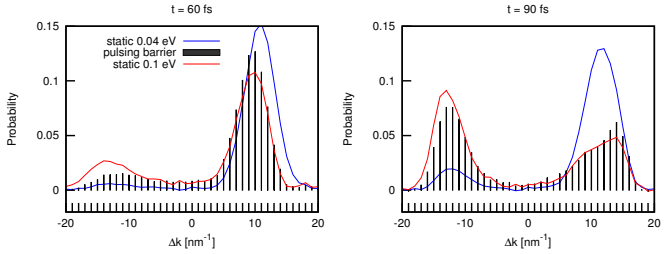

Figure 6. Comparison of the k-distributions (obtained by WMC) of the pulsating barrier and the static barriers of the limiting cases, as in Fig.5.

IV. Conclusion

The presented benchmark tests show that the WMC method has been matured to the point of providing highly accurate results, thanks to appropriate handling of the particle-generation statistics. In addition, practical issues which arise when using WMC to simulate semiconductor devices, e.g. time-varying potentials and an externally applied voltage between the contacts, have been treated. Moreover, all the presented considerations conceptually extend to higher dimensions and the method underlying the WMC simulator has already been shown to be numerically feasible in two dimensions [13], thereby paving the way for the accurate simulation of mesoscopic semiconductor devices using the Wigner formalism.

Acknowledgement

This work has been supported by the Austrian Science Fund, project FWF-P21685-N22.

References

[1] Y. Fu and M. Willander, "Electron wave-packet transport through nanoscale semiconductor device in time domain," *Journal of Applied Physics*, vol. 97, no. 9, p. 094311, 2005.

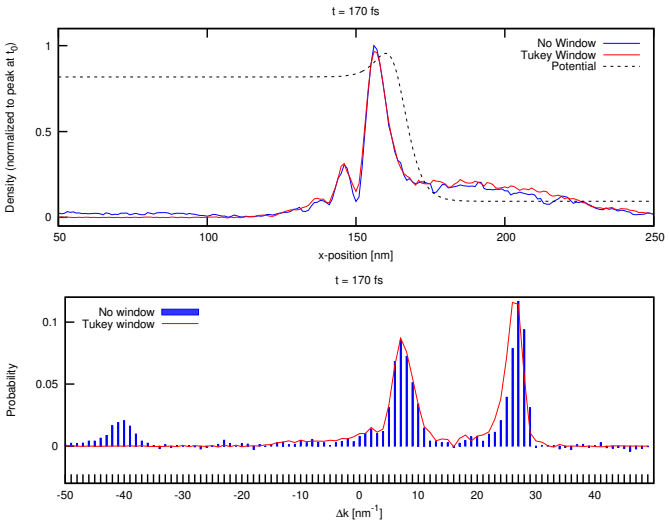

Figure 7. Wave packet traveling along a potential profile, of a biased device, showing a non-physical reflection and negative densities in the k-distribution arising, if no window is applied when calculating the Wigner potential.

[2] S. M. Amoroso, L. Gerrer, A. Asenov, J. M. Sellier, I. Dimov, M. Nedjalkov, and S. Selberherr, "Quantum insights in gate oxide charge-trapping dynamics in nanoscale MOSFETs," in *Proc. of the 18th Intl. Conf. on Simulation of Semiconductor Processes and Devices (SISPAD)*, pp. 25–28, 2013.

[3] D. Querlioz, J. Saint-Martin, A. Bournel, and P. Dollfus, "Wigner Monte Carlo simulation of phonon-induced electron decoherence in semiconductor nanodevices," *Phys. Rev. B*, vol. 78, p. 165306, Oct 2008.

[4] C. Jacoboni and P. Bordone, "The Wigner-function approach to non-equilibrium electron transport," *Reports on Progress in Physics*, vol. 67, no. 7, p. 1033, 2004.

[5] P. Wojcik, B. J. Spisak, M. Woloszyn, and J. Adamowski, "Self-consistent Wigner distribution function study of gate-voltage controlled triple-barrier resonant tunnelling diode," *Semiconductor Science and Technology*, vol. 24, no. 9, p. 095012, 2009.

[6] M. Nedjalkov, S. Selberherr, D. Ferry, D. Vasileska, P. Dollfus, D. Querlioz, I. Dimov, and P. Schwaha, "Physical scales in the Wigner-Boltzmann equation," *Annals of Physics*, vol. 328, pp. 220–237, 2012.

[7] M. Nedjalkov and D. Vasileska, "Semi-discrete 2D Wigner-particle approach," *Journal of Computational Electronics*, vol. 7, no. 3, pp. 222–225, 2008.

[8] I. T. Dimov, *Monte Carlo Methods for Applied Scientists*. World Scientific, 2008.

[9] M. Nedjalkov, P. Schwaha, S. Selberherr, J. M. Sellier, and D. Vasileska, "Wigner quasi-particle attributes – An asymptotic perspective," *Applied Physics Letters*, vol. 102, no. 16, pp. –, 2013.

[10] V. Los and N. Los, "Exact solution of the one-dimensional time-dependent Schrödinger equation with a rectangular well/barrier potential and its applications," *Theoretical and Mathematical Physics*, vol. 177, no. 3, pp. 1706–1721, 2013.

[11] P. Ellinghaus, M. Nedjalkov, and S. Selberherr, "Efficient calculation of the two-dimensional Wigner potential," in *Abstracts of the 16th Intl. Workshop on Computational Electronics (IWCE)*, pp. 19–20, 2014.

[12] P. Ellinghaus, M. Nedjalkov, and S. Selberherr, "Implications of the coherence length on the discrete Wigner potential," in *Abstracts of the 16th Intl. Workshop on Computational Electronics (IWCE)*, pp. 155–156, 2014.

[13] J. M. Sellier, M. Nedjalkov, I. Dimov, and S. Selberherr, "Two-dimensional transient Wigner particle model," in *Proc. of the 18th Intl. Conf. on Simulation of Semiconductor Processes and Devices (SISPAD)*, pp. 404–407, 2013.